Impact of Laser Mode Partition Noise on Optical Heterodyning at Millimeter-Wave Frequencies

Hamza Hallak Elwan, Ramin Khayatzadeh, Tong Shao, Julien Poette, Beatrice Cabon, Liam P. Barry

Impact of Laser Mode Partition Noise on Optical Heterodyning at Millimeter-Wave Frequencies

Hamza Hallak Elwan[1], Ramin Khayatzadeh[1], Tong Shao[2], Julien Poette[1], Beatrice Cabon[1], and Liam P. Barry[2], *Senior Member, IEEE*

***Abstract*—This paper examines the impact of laser mode partition noise (LMPN) during optical heterodyning process. The system presented here employs a passively mode-locked laser diode (PMLLD) as a multi-mode source for millimeter-wave (mm-wave) generation. A comprehensive theoretical and experimental study of LMPN at low frequency and, for the first time, in mm-wave frequency band is demonstrated. Simulations are presented to investigate the distribution of mode partition noise across optical modes. LMPN appears as an impairment in performance on a radio-over-fiber (RoF) communication system by increasing the intensity noise when the number of optical modes detected by a photodiode (PD) is limited. The effect of LMPN for various number of modes is demonstrated by coherent and incoherent receivers, and it is shown that 25 dB degradation in signal power occurs due to noise when not all modes are detected.**

***Index Terms*—Error vector magnitude (EVM), laser mode partition noise (LMPN), millimeter-wave (mm-wave), optical heterodyne, passively mode-locked laser diodes (PMLLD), phase noise, radio-over-fiber (RoF), relative intensity noise (RIN).**

I. Introduction

THE push towards very high bit rate wireless communication systems requires substantial spectral bandwidth. This has motivated the use of millimeter-wave (mm-wave) frequencies [1] and in particular, the unlicensed band from 57 to 64 GHz [2],[3]. Wireless communications in this frequency band are employed for short distance or indoor systems due to enormous attenuation in the atmosphere at 60 GHz [4]. Therefore, the prominent interest in microwave photonic generation of mm-wave signals such as optical heterodyning is growing rapidly [5],[6], where two or more optical modes beat on a high-speed photodiode (PD). An optical fiber is used to transmit the generated optical signals and data from the central station (CS) to the base station (BS), and owing to heterodyne process on PD, the electrical mm-wave signals are generated before distribution to mobile stations.

Optical sources employed in mm-wave radio-over-fiber (RoF) communication system generate optical noise which degrades the system performance. Optical noise predominantly originates from laser dynamics and spontaneous emission that induce fluctuations in both amplitude and phase of the optical source field. For two independent semiconductor lasers with linewidths of several MHz, this exhibits in large phase noise on the RF beat signal. A mode-locked laser diode (MLLD) can be employed for heterodyne mm-wave generation, and thanks to mode locking and correlation of phase noise between the optical lines. This source does not require any external locking scheme to partially alleviate phase noise on RF signals [7]-[9], which results in better system stability and cost efficient mm-wave generation [10]. The influence of phase noise on mm-wave and sub-THz RoF system was investigated [11]-[13]. We also demonstrated the impact of relative intensity noise (RIN) on the generation of mm-wave signals for two different kinds of lasers, and an envelope detector (ED) was proposed to only detect the intensity noise on mm-wave [14]-[16] and W band signals [17]. The use of multi-mode sources can lead to larger power fluctuations in each mode due to laser mode partition noise (LMPN) with relatively constant total optical power from source. When filtering a single optical mode of multi-mode laser, LMPN results the in poor system performance for data transmission and communication links [18], but LMPN is neglected for the entire optical spectrum since intensity fluctuations are eliminated on optical lines [19],[20].

In this paper, LMPN is both theoretically and experimentally studied in order to characterize the power fluctuation among optical modes and its impact on mm-wave frequency band. Therefore, a 60 GHz RoF system employing a passively mode-locked laser diode (PMLLD) is investigated with two different receivers used for electrical detection: an RF coherent receiver using a mixer, and an incoherent receiver using an envelope detector. Simulations of mode partition noise are provided to clearly understand the LMPN distribution between different optical modes. Experimental measurements have been realized and are in a good agreement with simulation results. With increase in a number of modes, the LMPN impact decreases, however, the chromatic dispersion instigated due to increase in a number of modes, degrades the performance of 60 GHz RoF system. The influence of LMPN on error vector magnitude (EVM) is evaluated at a data rate of 100 Mbps quadrature phase shifting keying (QPSK) modulation format at a 60 GHz carrier.

This paper is organized as follows: section II presents theoretical analysis of LMPN. In section III, experimental setup, simulation of LMPN, and measured results at both low and mm-wave frequency are discussed. Section IV investigates the transmission experiment and LMPN impact on EVM at 60 GHz, and a conclusion is provided in section V.

The authors (1) are with Grenoble Alpes University, Institut de Microélectronique Electromagnétisme et Photonique-LAboratoire d'Hyperfréquences et de Caractérisation, IMEP-LAHC, F-38000 Grenoble, France (e-mail: hamza.hallak-elwan@imep.grenoble-inp.fr; khayatzr@minatec.inpg.fr; julien.poette@phelma.grenoble-inp.fr; beatrice.cabon@grenoble-inp.fr).

The authors (2) are with Radio and Optical Communication Lab, Rince Institute, Dublin City University, Dublin, Ireland (e-mail: tong.shao@dcu.ie; liam.barry@dcu.ie).

II. Theoretical Analysis of LMPN

The principle of generating mm-wave signals through optical heterodyning requires beating of at least two optical tones on a PD with a frequency difference between modes equals to the desired mm-wave frequency. The electrical field $E(t)$ of a multi-mode laser, (M) modes, can be defined as:

$$E(t) = \sum_{i=1}^{M} A_i \Big(1+\gamma_i(t)+\psi_i(t)\Big) \exp\Big(j\big(2\pi\big(f_0+if_r)t+\phi_i(t)\big)\Big) \quad (1)$$

where A_i, $(\gamma_i+\psi_i)$, and ϕ_i are field amplitude, total amplitude noise, and phase noise of ith optical mode, respectively. f_0 is the carrier frequency of first mode, and f_r is the beating frequency corresponding to the free spectral range (FSR) of laser. The total amplitude noise is sum of relative intensity noise (RIN) expressed from laser rate equations which is represented by (γ_i) and laser mode partition noise (LMPN) expressed by (ψ_i). Since the repetition frequency (f_r) of PMLLD used is 58.63 GHz, the spectral terms of frequency equal or higher than $(2f_r)$ are filtered out by PD of 70 GHz bandwidth. After some simple manipulations, the photodetected current $I(t)$ for (M) modes can be expressed as:

$$I(t) = \sum_{i,j}^{M} \alpha\sqrt{I_i I_j} \times \Bigg[\Big(1 + (\gamma_i(t) + \gamma_j(t)) + (\psi_i(t)+ \psi_j(t))\Big) \cos\Big(2\pi(f_j - f_i))t + (\phi_j(t) - \phi_i(t))\Big)\Bigg] \quad (2)$$

where I_i is DC photodetected current for ith mode, (f_j-f_i) is mm-wave frequency of the generated beating between modes i and j, and $(\phi_j - \phi_i)$ is phase noise exhibited on the mm-wave carrier. For $(i=j)$, $\alpha = 1$ and first sum in (2) is the total DC current from sum of each DC contribution from each mode while second sum $(\gamma_i + \gamma_j)$ and third sum $(\psi_i + \psi_j)$ represent RIN and LMPN from DC to a few GHz, respectively. Whenever $(i\neq j)$, $\alpha = 2$, first term is sum of all beating terms. Second sum corresponds to RIN contribution of beating term at frequency of $(f_j - f_i)$, while third sum is associated to noise partition effect of beating between modes i and j. In (2), second order terms of RIN and LMPN have been neglected.

In order to calculate power spectral density (PSD) of the detected photocurrent, auto-correlation function $R_I(\tau)$ of the photocurrent is derived, assuming the fluctuations of amplitude noise are stationary [21]. Using the small angle approximation, $R_I(\tau)$ can be defined as:

$$R_I(\tau) = \Big\langle I(t)I(t+\tau)\Big\rangle = \Bigg\langle \sum_{i,j=1}^{M}\sum_{m,n=1}^{M} \alpha^2\sqrt{I_iI_j}\sqrt{I_mI_n} \times A_{i,j,m,n}(t,t+\tau)\,\phi_{i,j,m,n}(t,t+\tau)\Bigg\rangle \quad (3)$$

where $\langle\rangle$ is mean value over time, and τ is a positive time delay in realistic system. Whereas each beating corresponds to interaction between 2 optical modes, four indexes are used in this equation to represent the correlations between the beatings of pairs of modes. Consequently, correlation with indexes i, j, m, n is associated with beating between modes i and j and beating between modes m and n. $A_{i,j,m,n}(t,t+\tau)$ and $\phi_{i,j,m,n}(t,t+\tau)$ are correlations of amplitude noise and phase noise of beatings produced by modes (i,j) and (m,n), respectively. In case where both amplitude and phase noise of the mm-wave signal are uncorrelated, separate averages can be considered on both amplitude and phase noise. Therefore, the average of amplitude noise correlation can be derived after neglecting the mean value of amplitude noise of a specific mode, $\langle\gamma\rangle = \langle\psi\rangle = 0$. According to laser dynamic, RIN is produced up to a few GHz, limited by the relaxation frequency of laser. Due to coupling between modes, power fluctuation among longitudinal modes causes mode partition noise [18]-[20],[22]. Therefore, RIN and LMPN can be considered as having independent origins, and subsequently their correlation functions are neglected in this approach $\langle\gamma\times\psi\rangle = 0$. The average of amplitude noise correlation can be expressed as:

$$\begin{aligned}\big\langle A_{i,j,m,n}(t,t+\tau)\big\rangle = \Big\langle 1 &+ \gamma_i(t)\gamma_m(t+\tau) + \gamma_i(t)\gamma_n(t+\tau) \\ &+ \gamma_j(t)\gamma_m(t+\tau) + \gamma_j(t)\gamma_n(t+\tau) + \psi_i(t)\psi_m(t+\tau) \\ &+ \psi_i(t)\psi_n(t+\tau) + \psi_j(t)\psi_m(t+\tau) + \psi_j(t)\psi_n(t+\tau)\Big\rangle \end{aligned} \quad (4)$$

For $(i = m$ and $j = n)$, summation of auto-correlation functions are linked to amplitude noise on individual modes while for all other cases, summation of cross-correlation functions are related to amplitude noise among different modes i.e. beatings. From (2), (3), and (4), classical definition of RIN and LMPN of the beating between modes i and j are linked to the parameters $\psi_{i,j}$ and $\gamma_{i,j}$ using:

$$RIN_{ij}(t,t+\tau) = 4\gamma_i(t)\gamma_j(t+\tau) \quad (5)$$

$$LMPN_{ij}(t,t+\tau) = 4\psi_i(t)\psi_j(t+\tau) \quad (6)$$

The average of phase noise correlation can be expressed as:

$$\big\langle \phi_{i,j,m,n}(t,t+\tau)\big\rangle = \frac{1}{2}\Bigg\langle \cos(2\pi(f_n - f_m)\tau) + \Big(\big(\Delta\phi_{i,j}(t) - \Delta\phi_{m,n}(t+\tau)\big)\Big)\sin(2\pi(f_n - f_m)\tau)\Bigg\rangle \quad (7)$$

The PSD of the detected photocurrent $S_I(f)$ can be calculated by the Fourier transform of its auto-correlation in (3):

$$S_I(f) = \frac{1}{2}\sum_{i,j,m,n} \alpha^2\sqrt{I_iI_jI_mI_n}\Bigg(\Big(A_{i,j,m,n}(f)\times\delta\left[2\pi(f_n - f_m)\right]\Big) + \langle G_{A,\phi}(f)\rangle \times \delta\left[2\pi(f_n - f_m)\right]\Bigg) \quad (8)$$

where δ is the dirac function, and,

$$A_{i,j,m,n}(f) = FT\big[\langle A_{i,j,m,n}(t,t+\tau)\rangle\big]$$

$$G_{A,\phi}(f) = FT\Big[\big\langle A_{i,j,m,n}(t,t+\tau)\times\Big(\Delta\phi_{i,j}(t) - \Delta\phi_{m,n}(t,t+\tau)\Big)\big\rangle\Big]$$

When intensity noise and phase noise are considered statistically independant, this expression can be simplified as:

$$\Big\langle A_{i,j,m,n}(t,t+\tau)\times\Big(\Delta\phi_{i,j}(t) - \Delta\phi_{m,n}(t,t+\tau)\Big)\Big\rangle = \Big\langle A_{i,j,m,n}(t,t+\tau)\Big\rangle \times \Big\langle\Big(\Delta\phi_{i,j}(t) - \Delta\phi_{m,n}(t,t+\tau)\Big)\Big\rangle \quad (9)$$

It can be observed from (8) that the impact of both RIN and LMPN for a multi-mode laser degrades the performance of RoF system at baseband and mm-wave frequencies by generating intensity noise through parameters $A_{i,j,m,n}$.

III. Experimental Investigation of LMPN at Low Frequency and at Millimeter-Wave Band

This section experimentally analyzes and examines the impact of laser mode partition noise on baseband and mm-wave frequency band. The electrical power spectrum distribution of LMPN is measured for different number of optical modes using an optical filter. This study is implemented in both (300 MHz-18 GHz) and mm-wave frequency ranges.

A. Experimental Setup

The configuration of the experimental setup for LMPN analysis is shown in Fig. 1. PMLLD generating a low phase noise signal at 58.63 GHz by heterodyning is used. Considering chromatic dispersion effect, optimum length of 72m single mode optical fiber (SMF) G.652 is added to obtain the maximum electrical power of mm-wave signal. For identifying the impact of LMPN, number of detected modes is varied by filtering optical tones using a wavelength selective switch (WSS) employed as a wave shaper 1000S programmable optical filter from Finisar to select limited number of optical tones at point (b). For investigating LMPN at baseband and mm-wave frequencies, two different paths are used.

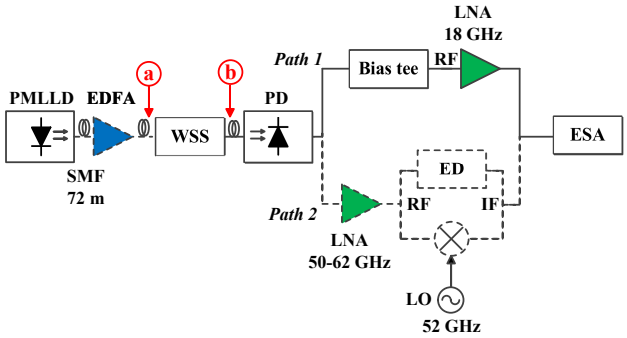

Fig. 1. Schematic of experimental setup for RoF system based on PMLLD, components indicated in dash line are used for mm-wave band.

The first detection system (path 1) is dedicated to low frequency analysis in (300 MHz-18 GHz) frequency range as uses a bias tee of (0.3-26.5) GHz bandwidth for suppressing the DC component, and a 40 dB gain amplifier having a 18 GHz bandwidth. The second detection system (path 2) is used for mm-wave measurements where a 19.5 dB gain erbium-doped fiber amplifier (EDFA) after a PMLLD is employed when reducing the number of modes. In path 2, a 35 dB gain amplifier in (50-62) GHz range is used and the amplified mm-wave signal is passed to a mixer or an envelope detector. When using the mixer, a local oscillator (LO) at 52 GHz down-converts mm-wave signal to 6.63 GHz. Since an envelope detector only detects intensity, the noise detected is due to sum of RIN and LMPN in a PSD of photocurrent, and thus there is no impact of phase noise on beating signal [15],[16]. In both schemes, Anritsu electrical spectrum analyzer (ESA) is then used to measure the PSD of the photodetected current.

The optical spectrum at point (a) of Fig. 1 is presented in Fig. 2 (a) measured by an optical spectrum analyzer (OSA) of 0.05 nm resolution bandwidth, showing a very large number of modes with a flat amplitude distribution. The instances of optical spectrum at point (b) are shown in Fig. 2: when filtering two modes in (b.1), when filtering seven modes in (b.2), or when detecting all modes except its left side modes at lower power in (b.3).

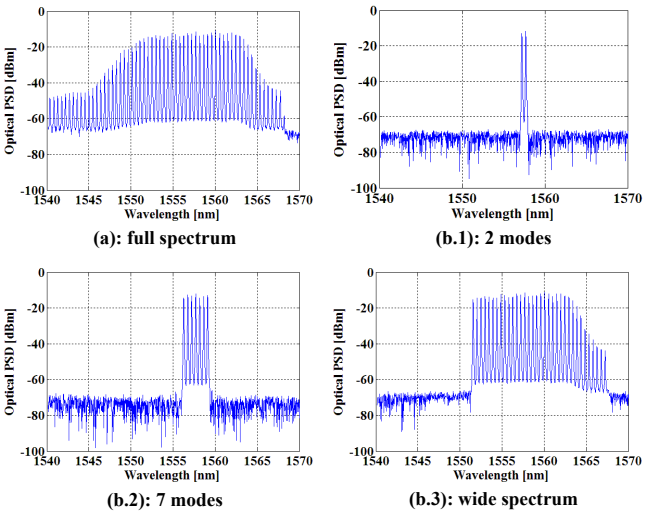

Fig. 2. Optical spectrum of PMLLD for different bandwidth of WSS at biased current 209 mA.

In experimental measurements, thermal noise of the system and shot noise have been measured, and their contributions have been de-correlated from experimental results because they have different and independent physical origins from LMPN [23]. After measuring S parameters of the opto-electric (O/E) system by a vector network analyzer (VNA), frequency response of detection system from photodiode to ESA has been accounted for in results.

B. Mode Partition Noise Simulation and Distribution

After theoretical analysis of LMPN in section II, the simulation is described here to highlight noise behavior which depends on mode partition within the optical spectrum. The number of beating contributions is $(M-1)$, but LMPN influences all modes, and therefore it possesses (M) contributions. Simulations are conducted using the MathWork's MATLAB software. From theoretical analysis of LMPN expressed in section II, there are two contributions:

1) Noise Contribution from Each Mode: In optical comb, each mode (i) has its own contribution (ψ_{ii}) to the noise induced by mode partition. Its level mainly depends on average optical mode power. The noise due to mode partition on a given mode (i) is compensated by sum of noise (ψ_{ji}) induced by mode (i) on other modes (j). The summation of (ψ_{ii}) and (ψ_{ji}) is therefore equal to zero, as can be described:

$$\psi_{ii} + \sum_{j \neq i}^{M} \psi_{ji} = \sum_{j=1}^{M} \psi_{ji} = 0 \qquad (10)$$

Whenever (ψ_{ii}) is positive or negative, (ψ_{ji}) contribution will be opposite in this model. Different distributions of this compensation can be considered: compensation across the entire spectrum (first scenario) or over a limited number of neighboring modes (second scenario).

2) Total LMPN of Mode (i): The influence of other modes (j) produces contributions (ψ_{ij}) on a given mode (i). From mathematical analysis, the contribution (ψ_{ii}) represents auto-correlation function of mode partition for mode (i) while the contributors (ψ_{ji}) and (ψ_{ij}) correspond to cross-correlation function of mode partition between mode (i) and mode (j), respectively. The total noise ψ_i due to mode partition of a given mode (i) is sum of its own contribution (ψ_{ii}) and contribution (ψ_{ij}) from other modes (j), expressed as:

$$\psi_i = \psi_{ii} + \sum_{j \neq i}^{M} \psi_{ij} = \sum_{j=1}^{M} \psi_{ij} \tag{11}$$

Table I describes an example of LMPN distribution between 3 optical modes. According to (10), sum of terms in each column should equal zero, while from (11), sum of all the terms in each row gives the total mode partition noise of the concerned mode $\psi_i \neq 0$.

Impact of	mode 1	mode 2	mode 3	Line sum
On mode 1	ψ_{11}	ψ_{12}	ψ_{13}	ψ_1
On mode 2	ψ_{21}	ψ_{22}	ψ_{23}	ψ_2
On mode 3	ψ_{31}	ψ_{32}	ψ_{33}	ψ_3
Column sum	0	0	0	0

TABLE I
DISTRIBUTION LMPN ACROSS THREE OPTICAL MODES

Table I shows that when all modes are detected, the total contribution of mode partition on noise $\psi_1 + \psi_2 + \psi_3$ equals zero, and consequently no impact of mode partition can be seen. The following simulation parameters have been selected as follows to correspond to the experimental investigation: the number of modes (M) of the optical spectrum is 41, and non-normalized mode powers I_i are considered to exhibit the effects of power spectrum distribution. Fig. 3 represents the experimental measurements and simulation results of LMPN at low frequency where curves describe the cumulative power of LMPN versus an increasing number of detected modes. Curve (1) illustrates experimental measurements of mode partition obtained in (300 MHz-18 GHz) using path 1 of Fig. 1, and simulation results in curves (2) and (3) are performed for a random LMPN distribution. The difference between two simulation curves (2) and (3) in Fig. 3 depends on the distribution of noise: noise from one mode (i) can be distributed over all modes (curve 2) or on a limited number of modes (6 modes here for curve 3).

Curve (2) increases as a function of number of modes to reach a maximum for 15 modes and then decreases to 0 when all modes are aggregated. It is important to notice that accumulation of more than 27 modes modifies the curve slope due to integration of side modes that have a reduced power compared to others central modes. Curve (3) corresponds to a distribution of noise over only 6 neighboring modes.

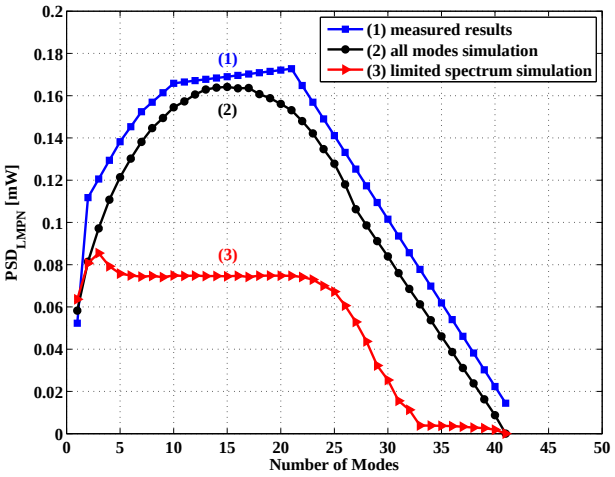

Fig. 3. LMPN of measurements and simulation results with different LMPN distribution between optical modes.

Simulation results shown in curve (2) where noise is distributed over all modes is in close agreement with experimental measurements of curve (1). This indicates that all modes, even those having low power like side modes, need to be detected in order to suppress the effect of mode partition. It can be concluded that, in this study, noise is experimentally distributed over all modes.

C. LMPN Effects in (300 MHz-18 GHz) Frequency Range

For measurements of mode partition noise at low frequency, experiments has been carried out using path 1 of Fig. 1. In this case, EDFA is not used, and the total optical power of 9 dBm is used. Fig. 4 depicts the PSD normalized to optical power of detected signal in (300 MHz-18 GHz) for different number of optical modes detected, but displayed up to 7 GHz for better clarity. This normalization is performed to compensate optical power increase when detecting a larger number of modes.

Noise measured for frequencies lower than 300 MHz is due to detection stage, and therefore, it should not be considered here. LMPN is responsible for noise increase as high as 25 dB from 300 MHz to 2 GHz. In this experiment, WSS selects a specific number of optical modes that have different optical powers. Fig. 4, curve (1) shows that the normalized PSD of noise is maximum when detecting only one optical mode. LMPN contribution decreases proportionally to number of modes selected and reaches a minimum when all modes are selected. Fig. 4 reveals the minimum level of LMPN can be achieved and corresponds to the noise floor level of system when all optical modes (41 modes) are in WSS bandwidth.

In mm-wave RoF system of Fig. 1, an EDFA is used to compensate for optical power losses when selecting a small number of modes by WSS. In order to study the effect of amplified spontaneous emission (ASE) noise induced by EDFA, we have carried out experiments with, and without, EDFA at low frequency (path 1 of Fig. 1). The measured PSD is depicted in Fig. 5 with EDFA (curves (1) and (2)) and without EDFA (curves (3) and (4)). The comparison is made for 2 cases: for only 2 modes, curves (1) and (3) and for all

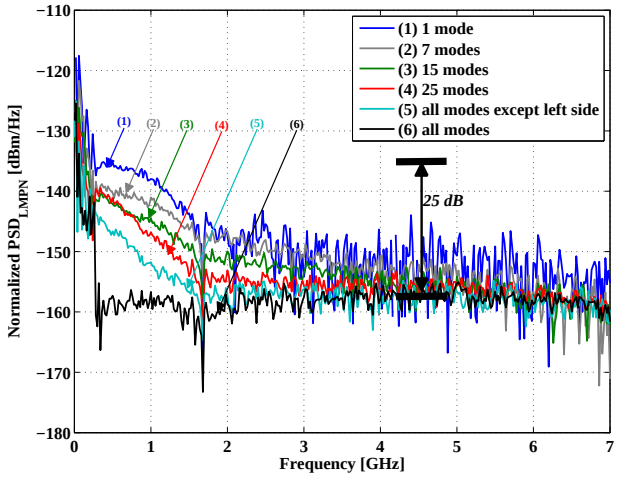

Fig. 4. The PSD of LMPN as a function of frequency for a different number of optical modes.

modes (curves (2) and (4)). For 2 modes case, the contribution of mode partition on PSD can be clearly identified by noise increase in frequency range below 2 GHz.

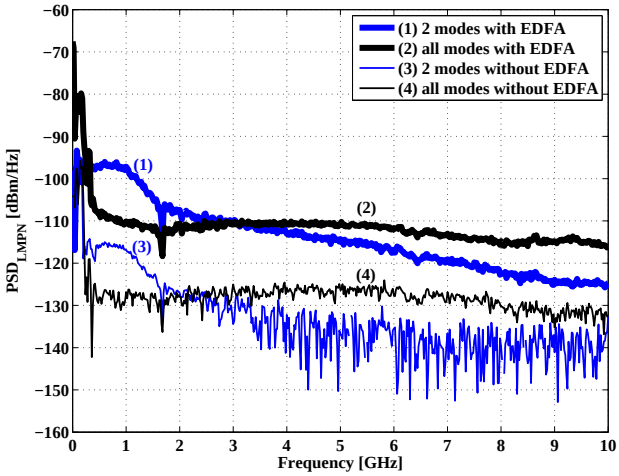

Fig. 5. The PSD comparison between experiments using EDFA and experiments without EDFA for two optical modes and all optical modes.

It can be noticed in Fig. 5 that the measured PSD results, with and without EDFA, have the same behavior but differ by 19.5 dB corresponding to EDFA gain. Therefore, there is no additional degradation of noise thanks to good saturation of EDFA and a WSS employed after EDFA.

D. LMPN Effects in mm-wave RoF System

An investigation of laser mode partition noise on mm-wave signals is performed. Fig. 1, path 2 describes the schematic diagram of experimental setup using both coherent and incoherent receivers, for a total optical power of 9 dBm. EDFA is used to compensate for optical losses induced by optical filtering performed by the WSS when selecting different number of optical modes.

For coherent receiver, an LO signal of 52 GHz is applied to a mixer for down-conversion as represented in path 2 of Fig. 1. Since phase noise of LO is extremely low (-140 dBc/Hz for frequency offset above 10 MHz) [24], the influence of phase noise of mixing process on IF signal is neglected.

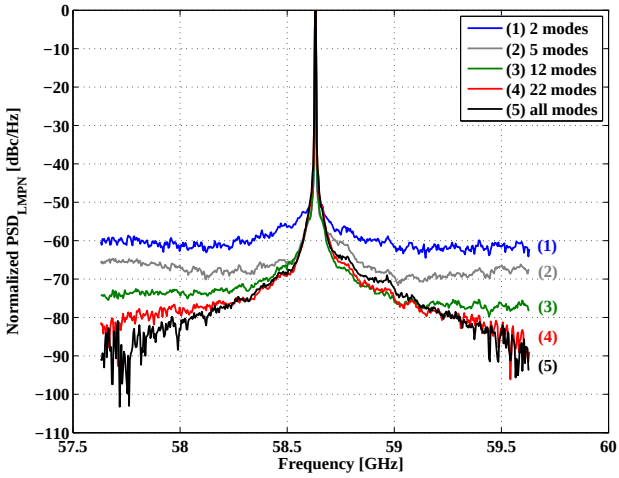

Fig. 6. The normalized mode partition noise PSD of un-modulated mm-wave signal based on mixer.

Fig. 6 illustrates electrical power spectrum density of received mm-wave signals normalized to mm-wave carrier for various optical bandwidth of WSS. It can be observed from the linewidth of mm-wave signals that phase noise is reasonably constant while the LMPN has different levels. This confirms that intensity noise from mode partition can be observed on mm-wave carrier and degrades the system performance. For non-normalized PSD and with an increasing number of modes, LMPN would slowly increase with increase in power of RF carrier. Measurements in Fig. 6 clearly indicate that LMPN contribution decreases when optical spectrum is extended, and thus the behavior of mode partition noise at mm-wave signal is comparable to that at low frequency as shown in Fig. 4.

When using incoherent receiver, with an envelope detector, the solely amplitude noise impact is measured and investigated. The detected normalized PSD of mode partition noise is depicted in Fig. 7 after detection. Measurements are implemented for an optical photodetected power of 0 dBm with different number of modes in optical spectrum. Due to limited bandwidth of Schottky diode used, results are presented up to 2 GHz. A good agreement with results of Fig. 4 is obtained: when all modes are detected, the impact of noise mode partition is minimal. Here, curve (5) in Fig. 7 corresponds to a residual amplitude noise which only originates from RIN, which is filtered out by ED response. Similar result can be observed by detecting a signal in a system where no mode partition noise exists, measuring beating between two independent mono-mode lasers, e.g. distributed feedback laser [15],[16].

Fig. 7 clearly shows an increase of mode partition noise detected in mm-wave frequency band when reducing number of optical modes. We can conclude that LMPN also influences amplitude noise on mm-wave signals, as described in (8), and

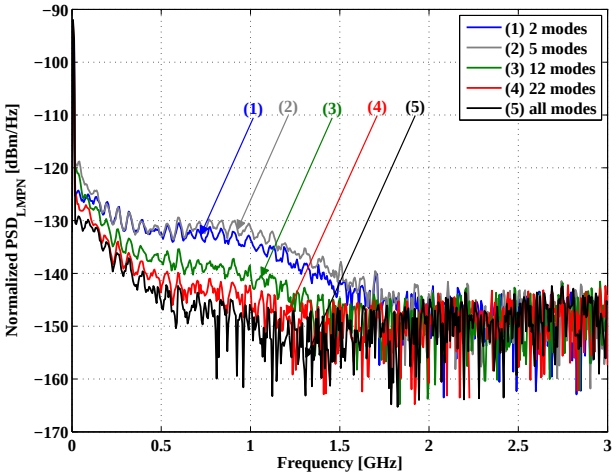

Fig. 7. The normalized mode partition noise PSD of un-modulated mm-wave signal after down-conversion based on envelope detector.

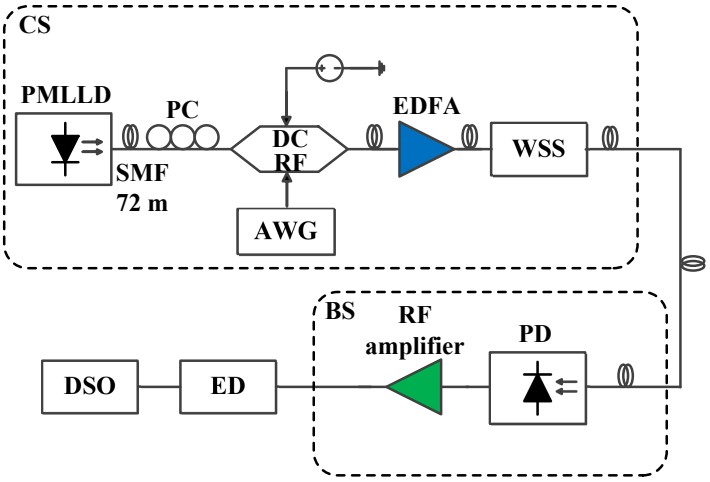

Fig. 8. The configuration of experimental setup for 60 GHz RoF communication system based on incoherent receiver.

degrades system performance. The heterodyne process induces LMPN in generated signal, even at mm-wave frequency.

IV. Digital Modulation Experiment of 60 GHz RoF Transmission

We have then analyzed the effect of LMPN on EVM for 60 GHz RoF system with digital modulation.

A. Experimental Setup

The schematic diagram of experimental setup used to investigate system performance is presented in Fig. 8 for 100 Mbps QPSK modulation at 1 GHz subcarrier onto mm-wave carrier for analysis of LMPN impact on EVM. In the central station (CS), the previous PMLLD is utilized, and the same SMF length of 72 m is used as before. A polarization controller (PC) is added to adjust polarization state of optical signal. A Mach-Zehnder modulator (MZM) biased at quadrature point is employed for applying data stream from an arbitrary waveform generator (AWG). An EDFA is used for compensation of modulator losses and optical power variation when reducing the optical spectrum bandwidth using WSS. WSS is designated to filter out some modes from optical comb and to control transmitted optical power since it can also be used as an optical attenuator. For a fiber-optic transmission, the base station (BS) detects optical signal on a high-speed PD where the heterodyne mm-wave signal is generated at 58.63 GHz. This signal is amplified by an RF amplifier before being detected using ED.

Both down-converted signal and data are captured and sampled by a high-speed digital sampling oscilloscope (DSO) from Agilent 54855A of 6 GHz bandwidth. EVM is then evaluated in on-line from the measurements using a vector signal analyzer (VSA) installed on the DSO. More information can be found in [15],[16], where theory and mathematical equations of amplitude noise were discussed for a system based on an ED.

B. EVM Dependance on A Number of Modes

The measurements are carried out for EVM behavior at 1 GHz subcarrier frequency of 60 GHz carrier. Fig. 9 depicts two cases where 2 optical modes are selected from flatness power modes using WSS (square points), or all modes are detected (circle points). For both cases, WSS also operates as a variable optical attenuator to control the received RF power.

From the measured PSD of mode partition noise using mixer of Fig. 6 and using an ED of Fig. 7, LMPN measurements for 2 modes demonstrate more influence than all modes. Thus, EVM of 2 modes is higher than all modes, as can be seen in Fig. 9. For 2 optical modes detected, the lowest EVM achieved is 8.1 % for a received RF power of -26.7 dBm. Since LMPN depends on an optical power, the same results are observed for other sets of two adjacent modes are considered where the optical lines are flat. When detecting the entire optical spectrum, EVM decreases to 6.2 % at the same received RF power. The EVM trends for 2 modes and entire spectrum are closely congruent. It can again be concluded that for reducing the impact of LMPN at baseband and on 60 GHz signals, it is shown that it is necessary to increase number of optical modes. Another solution could be a careful choice of the frequency subcarrier with respect to generated mm-wave carrier to avoid the effect of laser mode partition. When increasing fiber length, chromatic dispersion will induce a time delay between different beatings. This can be interpreted by a de-correlation between optical modes, and consequently noise induced by LMPN will be de-correlated as well. Therefore, this delay degrades the compensation of mode partition noise which can not fully be compensated when detecting several beatings. The frequency limit at which the compensation is possible depends on fiber length and wavelength difference between beatings, and number of beatings should also be considered.

For entire optical spectrum, we encounter a trade-off between laser mode partition noise and chromatic dispersion that both degrade system performance and limit the transmission length.

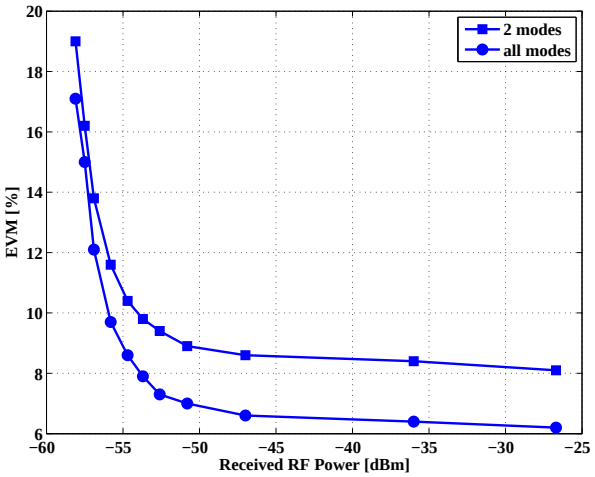

Fig. 9. Measured EVM as a function of received RF power for filtered two optical modes and entire optical spectrum at 100 Mbps of QPSK modulation.

V. Conclusion

We have studied and demonstrated the impact of laser mode partition noise on baseband and mm-wave RoF communication systems. Applications concern PMLLD possessing a low phase noise for generation of a beating signal. The study of LMPN performed on optical heterodyning has been investigated by theoretical analysis and experimental results, where simulations are implemented to describe the behavior of LMPN across the optical spectrum. Impact of LMPN on generated mm-wave carrier has been experimentally demonstrated. Very close agreement is found with measured results.

The experiments have been carried out on mm-wave RoF systems utilizing both coherent and incoherent receivers for down-conversion, and electrical spectrums of LMPN have been presented. EVM versus RF power is measured using data rates of 100 Mbps and QPSK modulation on 1 GHz subcarrier for the case of two filtered modes and the entire optical spectrum. The results conclude that, for a larger number of modes, LMPN impact is lowered. It is worth mentioning that even side modes of low power have a strong impact on LMPN level. Careful attention should be made when designing system to avoid partition noise effect that could degrade signal transmission and considering chromatic dispersion effect. We We would like to highlight that this study and the model can be applicable to any kind of optical heterodyne generation system.

Acknowledgment

The authors acknowledge that this work was co-funded by Ulysses Project, the French Ministry of Foreign Affairs and International Development (MAEDI) and French Ministry for High Education and Research (MENESR). The authors wish to thank III-V lab for providing the PMLLD chip.

References

[1] T. Kleine-Ostmann and T. Nagatsuma, "A review on terahertz communications research" *J. Infrared Millimeter Terahertz Waves*, vol. 32, pp. 143-171, Feb. 2011.

[2] N. Guo et al., "60 GHz millimeter-wave radio: principle, technology and new results" *Eurasip J. Wireless Communication Networks*, pp. 48-56, 2007.

[3] Su-Khiong Yong et al., "60 GHz Technology for GBPS WLAN and WPAN from theory to practice" *John Wiley and Sons, 2011.*

[4] P. Smulders, "Exploiting the 60 GHz band for local wireless multimedia access: prospects and future directions" *Communications Magazine, IEEE*, vol. 40, no. 1, pp. 140-147, 2002.

[5] Z. Jia et al., "Key enabling technologies for optical-wireless networks: optical millimeter-wave generation, wavelength reuse, and architecture" *IEEE J. Lightw. Technol.*, vol. 25, no. 11, pp. 3452-3471, Nov. 2007.

[6] A. Stohr et al.,"60 GHz radio-over-fiber technologies for broadband wireless services" *OSA J. Optical Networking*, vol. 8, no. 5, pp. 471-487, May 2009.

[7] F. Brendel et al., "PLL- stabilized optical communications in millimeter-wave RoF systems" *J. Opt. Commun. Netw.*, vol. 6, no. 1, pp. 45-53, Jan. 2014.

[8] B. A. Khawaja and M. J. Cryan, "Wireless hybrid mode locked lasers for next generation radio-over-fiber" *J. Lightw. Technol.*, vol. 28, no. 16, pp. 2268-2276, Aug. 2010.

[9] A. Stohr et al., "Millimeter-wave photonic components for broadband wireless systems" *IEEE Trans. Microw. Theory and Techn.*, vol. 58, no. 11, pp. 3071-3082, Nov. 2010.

[10] Ralf-Peter Braun et al., "Optical microwave generation and transmission experiments in the 12- and 60-GHz region for wireless communications" *IEEE Trans. Microw. Theory and Techn.*, vol. 46, no. 4, pp. 320-330, Apr. 1998.

[11] R. Khayatzadeh et al.,"Impact of phase noise in 60 GHz radio-over-fiber communication system based on passilevy mode-locked laser " *J. Lightw. Technol.*, vol. 32, no. 20, pp. 3529-3535, Oct. 2014.

[12] Criado, A. R., et al.,"Observation of phase noise reduction in photonically synthesized sub-THz signals using a passively mode-locked laser diode and highly selective optical filtering," *Optics express*, vol. 20, no. 2, pp. 1253-1260, 2012.

[13] Shao, Tong, et al.,"Phase Noise Investigation of Multicarrier Sub-THz Wireless Transmission System Based on an Injection-Locked Gain-Switched Laser," *Terahertz Science and Technology, IEEE Transactions*, vol. 5, no. 4, pp. 590-597, 2015.

[14] H. Hallak Elwan, R. Khayatzedeh, J. Poette, and B. Cabon, "Relative intensity noise in optical heterodyning applied to millimeter wave systems" *IEEE International Topical Meeting on Microwave Photonics, MWP 2015, Paphos, Cyprus, October 26-29*, doi:10.1109/MWP.2015.7356690, pp. 1-4, 2015.

[15] H. Hallak Elwan, R. Khayatzedeh, J. Poette, and B. Cabon,"Impact of Relative Intensity Noise on 60 GHz Radio-over-Fiber Wireless Transmission Systems millimeter-wave radio-over-fiber systems" *IEEE J. Lightw. Technol.*, Mar. 2016.

[16] R. Khayatzadeh, H. Hallak Elwan, J. Poette, and B. Cabon,"Impact of amplitude noise in millimeter-wave radio-over-fiber systems" *IEEE J. Lightw. Technol.*, vol. 33, no. 13, pp. 2913-2919, Jul. 2015.

[17] R. Khayatzedeh, H. Hallak Elwan, J. Poette, and B. Cabon, "100 GHz RoF System Based on Two Free Running Lasers and Non-coherent Receiver" *IEEE International Topical Meeting on Microwave Photonics, MWP 2015, Paphos, Cyprus, October 26-29*, doi:10.1109/MWP.2015.7356689, pp. 1-4, 2015.

[18] Robert H. Wentworth et al., "Laser mode partition noise in lightwave systems using dispersive optical fiber" *J. Lightw. Technol.*, vol. 10, no. 1, pp. 84-89, Jan. 1992.

[19] K. Ogawa , "Analysis of mode partition noise in laser transmission systems" *IEEE J. Quant. Electro.*, vol. QE-18, no. 5, pp. 849-855, May 1982.

[20] K. Ogawa and R. S. Vodhanel , "Measurements of mode partition noise of laser diodes" *IEEE J. Quant. Electro.*, vol. QZ-18, no. 7, pp. 1090-1093, Jul. 1982.

[21] H. A. Haus and A. Mecozzi, "Noise of mode-locked lasers" *IEEE J. Quantum Electron*, vol. 29, no. 3, pp. 983-996, Mar. 1993.

[22] Govind P. Agrawal, "Lightwave systems" in "Fiber-optic communication systems" *3rd ed., John Wiley & Sons*, 2002.

[23] J. Poette, et al.,"Highly sensitive measurement technique of relative intensity noise and laser characterization" *Fluctuation and noise letters: L81-L86*, 2008.

[24] Agilent E8257D PSG Microwave Analog Signal Generator Datasheet, *Agilent Technol*, Santa Clara, Ca, USA, 2012.